Action Potentials of Isolated Single Muscle Fibers Recorded by Potential-sensitive Dyes

SHIGEHIRO NAKAJIMA and ARIEH GILAI

From the Department of Biological Sciences, Purdue University, West Lafayette, Indiana 47907. A. Gilai's present address is Neurobiology Unit, Hebrew University, Jerusalem, Israel.

ABSTRACT Light transmission changes upon massive stimulation of single muscle fibers of *Xenopus* were studied with the potential-sensitive nonpermeant dyes, merocyanine rhodanine (WW375) and merocyanine oxazolone (NK2367). Upon stimulation an absorption change (wave *a*) occurred, which probably represents the sum of action potentials in the transverse tubules and surface membrane. In WW375-stained fibers wave *a* is a decrease in transmission over the range of 630 to 730 nm (with NK2367, over the range of 590 to 700 nm) but becomes an increase outside this range, thus showing a triphasic spectral pattern. This spectrum differs from that of the squid axon, in which depolarization produces only an increase in transmission over the whole range of wavelengths (Ross et al. 1977. *J. Membr. Biol.* **33**:141–183). When wave *a* was measured at the edge of the fiber to obtain more signal from the surface membrane, the spectrum did not seem to differ markedly from that obtained from the entire width of the fiber. Thus, the difference in the spectrum between the squid axon and the vertebrate muscle cannot be attributed to the presence of the tubular system.

INTRODUCTION

In this and the following paper we present results of experiments on potential-sensitive dyes applied to isolated single fibers of amphibian skeletal muscle. The main purpose of this investigation was to analyze the inward spread of muscle action potential along the transverse tubular system (T system) by this new technique (Tasaki et al., 1968; Cohen et al., 1970 and 1974).

There are two kinds of potential-sensitive dyes available: permeating or slow-response (e.g., carbocyanine dyes) and nonpermeating or fast-response (e.g., merocyanine rhodanine). The permeating dyes have the advantage that they produce a large signal, but also have a certain drawback: the dyes are known to produce two kinds of optical changes, fast signals and slow signals (the latter is called the redistribution signal) upon sudden changes of membrane potential (Cohen and Salzberg, 1978; Waggoner, 1979). In contrast, the nonpermeant dyes generally produce only rapid signals, and the optical signal occurs almost simultaneously with the potential change (Ross et al., 1977). (See Ross et al. [1977] for exceptions to this general rule.)

J. GEN. PHYSIOL. © The Rockefeller University Press · 0022-1295/80/12/0729/22 $1.00 729
Volume 76 December 1980 729–750

For this reason, we have used the nonpermeating, fast dyes, despite the fact that the signal size is rather small. When we started the experiments, the best fast-response dye available was merocyanine 540 (Cohen et al., 1974; Ross et al., 1974), and we used this dye in our series of preliminary experiments (Nakajima et al., 1976; Gilai and Nakajima, 1976). But later on, better fast-response dyes—merocyanine rhodanine and merocyanine oxazolone—became available (Grinvald et al., 1976; Ross et al., 1977), and thus we repeated and extended the experiments using these new dyes.

Potential-sensitive dye experiments on skeletal muscle have been carried out by several other groups of workers (Landowne, 1974; Oetliker et al., 1975; Bezanilla and Horowicz, 1975; Vergara and Bezanilla, 1976; Vergara et al., 1978; Baylor and Chandler, 1978; Baylor et al., 1979). But the main interest and emphasis of each group have been different. Our experiments are concerned only with the signals coming from the surface and the T-system membranes (not the ones from the sarcoplasmic reticulum). We have always used isolated single muscle fibers instead of fiber bundles, and we have sometimes compared the optical signals with intracellular action potentials in the same single muscle fiber.

In this paper a general description of dye-absorption signals will be given. The wavelength dependency of the signals will be treated in detail. It will be shown that the wavelength characteristics of muscle are different from those of the squid axon. In the following paper (Nakajima and Gilai, 1980) we will analyze the time-course of the optical signal in comparison with the electrical signal. Several preliminary accounts have been published (Nakajima et al. 1976; Gilai and Nakajima, 1976; Nakajima and Gilai, 1977 and 1978). Some of the results were presented at the Symposium on Excitation-Contraction Coupling at the University of California, Los Angeles (1979; proceedings in preparation).

METHODS

General Procedure

The experimental procedure was as follows: we isolated a single muscle fiber, stained it with merocyanine rhodanine (WW375) or merocyanine oxazolone, (NK2367) and measured optical transmission changes upon stimulation of the muscle fiber.

Single-twitch muscle fibers were isolated from the M. flexor brevis digitorum V (Ecker, 1971) of *Xenopus*. This muscle has fairly long tendons on both ends, and the muscle length (~5 mm) is suitable for our purposes. We have used *Xenopus* because it can be kept alive and healthy in the laboratory, thus ensuring a good supply of healthy muscles. The experimental chamber, resembling that of Hodgkin and Horowicz (1959), had a trough which measured 45 × 6 × 3 mm. Inside this trough the fiber was laid out and moderately stretched, and both tendons were pinned with fine needles onto two small silicone rubber pedestals. The trough was then covered with a microscope cover glass, thus forming a small tunnel. The solution inside this tunnel could be exchanged very rapidly with a minimum of dead space. The bottom of the trough was made of glass, through which the light entered the chamber and was focused on the muscle fiber. Both side walls of the trough were lined with platinum plates (14 × 3 mm), which were used as current electrodes for massive transverse stimulation.

The Ringer's solution contained: NaCl, 115 mM; KCl, 2.5 mM; $CaCl_2$, 1.8 mM; Na_2HPO_4, 2.15 mM; and NaH_2PO_4, 0.85 mM. The merocyanine rhodanine (WW375 or dye XVII of Ross et al. [1977]) has kindly been supplied by Dr. A. S. Waggoner, and merocyanine oxazolone (NK2367) was purchased from Nippon Kankoh-Shikiso Kenkyusho Co., Ltd., Okayama 700, Japan. Merocyanine 540 (dye I of Cohen et al. [1974]) was purchased from Eastman Kodak Co., Rochester, N. Y.

Diameter, *D*, refers to the width of muscle fiber stretched under experimental conditions as viewed by the microscope. All the experiments were conducted at room temperature.

Optical System

We followed the advice of Dr. L. B. Cohen in constructing the optical setup. The main component of the optical recording system (Fig. 1) was a Zeiss WL microscope (Carl Zeiss, Inc., New York). The incident light was provided by a halogen light source assembly (Zeiss) with a 100-W quartz-halogen bulb, the power being derived from a 12-V accumulator. The light was passed through two filters (*f1* and *f2* of Fig. 1). The second filter (*f2*) was an interference filter (Schott Optical Glass Inc., Duryea, Pa.; Balzers Corp., Nashua, N. H.; Feuer Associates, Upper Montclair, N. J.; or Corion Corp., Holliston, Mass.) with a half-height width usually ranging from 9 to 17 nm. The first filter (*f1*), a band-pass filter, served as a heat absorber. We used an RGN9 (Schott) when λ (the wavelength of the interference filter) was $\geqq$720 nm and a KG3 (Schott) when $\lambda < 720$ nm (see Ross et al., 1977). Sometimes an additional neutral density filter was inserted.

By using the condenser diaphragm (*c.d.*) the numerical aperture (NA) of the condenser was adjusted to 0.35, a value corresponding to the NA of the objective, and the illumination was carried out under Koehler's condition. An image of the muscle fiber was formed by a Zeiss objective (Fig. 1 *obj*; × 16; NA, 0.35), and at the level of the image a rectangular slit (*XY-diaph* in Fig. 1; Zeiss adjustable square diaphragm) was inserted to limit the light to a certain region of the fiber. The length and the width of the slit could be changed independently. The light coming from the slit converged through an eyepiece (*e.p.*) and then fell onto the active area (2.5 mm in diameter) of a photodiode (*p.d.* of Fig. 1; PV 100A, E G & G, Inc. Electro-Optics Div., Salem, Mass.). The optical assembly was placed on an air-cushioned experimental table.

To avoid unnecessary illumination, which might damage the fiber by photodynamic action, we inserted an electronic shutter (Uniblitz; Vincent Associates, Rochester, N.Y.) beneath the condenser. The shutter opened only during the time of recording. Typically the fiber was stimulated once every 2 s, and the shutter opened for only 200 ms of each 2-s period. The shutter was connected to a large stand, which was placed directly on the laboratory floor; this arrangement minimized the noise originating from the shutter movement.

Recording of Optical Signals

The output from the photodiode was fed into an *I-V* converter, and after passing through a direct current (*d.c.* in Fig. 1) offset voltage, the signal was fed into a balancing circuit (a sample-and-hold circuit with an extremely low droop rate) (Fig. 1). Changes in the optical signals were extremely small compared with the background light intensity. Thus, even a slight drift of the background light drove the oscilloscope beam off the scope screen. The function of the balancing circuit was to set the output dc voltage to zero level and hold it without distorting the signals (Nakajima et al., 1976). Once the output from the *I-V* converter was manually set to roughly zero by

the dc source, the balancing circuit worked in such a way that the dc output from the circuit was always zero. Input 2 to the pen recorder (Fig. 1) was to monitor the dc levels of the input to the balancing circuit. Input 1 to the pen recorder registered the actual dc level of the *I-V* converter output (i.e., the background light intensity).

Electrical Recording

In some experiments intracellular action potentials were recorded simultaneously with the optical signals. Glass capillary microelectrodes (6–7 MΩ; 3 M potassium acetate-filled) were used for intracellular recording. The electrical circuit for the microelec-

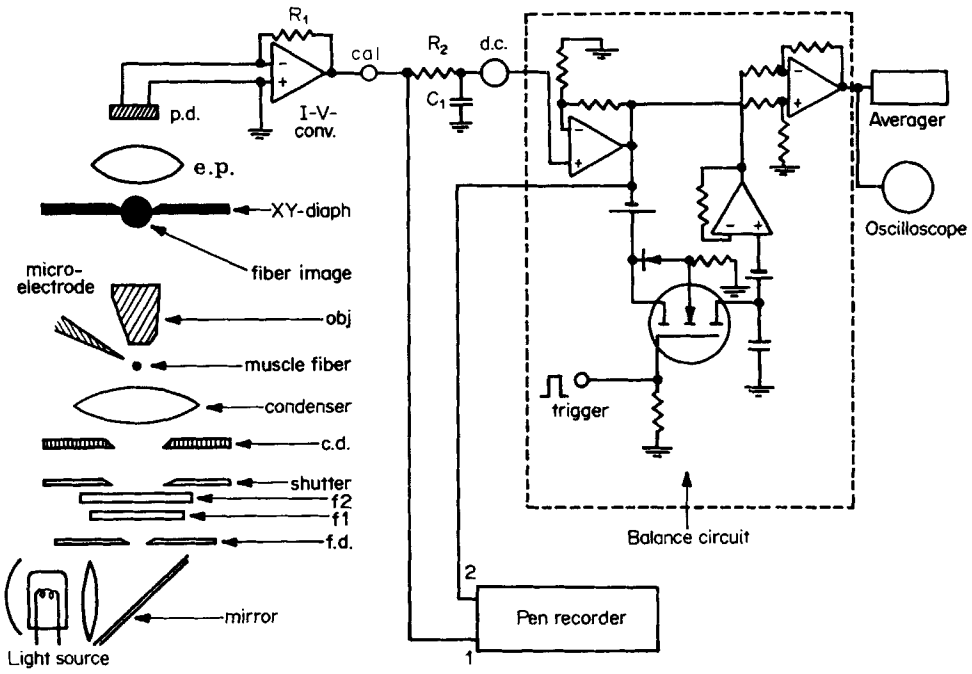

FIGURE 1. Schematic diagram of the photometry. *f.d.*, field diaphragm. *f1*, heat absorption filter. *f2*, interference filter. *c.d.*, condenser diaphragm. *obj*, microscope objective. *XY-diaph*, *X-Y* diaphragm. *e.p.*, eyepiece. *p.d.*, photodiode. *I-V-conv.*, *I-V*-converter. R_1, 2 MΩ. R_2, 3 kΩ. C_1, ~0.005 μF. *cal*, calibrator. *d.c.*, variable direct current voltage source. See the text for details.

trode was a conventional one, consisting of a negative capacity amplifier and an oscilloscope. For each experiment the negative capacity was adjusted to compensate for the input stray capacity. Then, the total frequency response of the electrical recording was made approximately the same as that of the optical recording by the use of a low-pass filter inserted between the amplifier and the oscilloscope. One of the difficulties with the electrical recording was a large shock artifact produced by the massive transverse stimulus. This was minimized by isolating the whole stimulus circuit from the ground and by using a fine Ag-AgCl electrode, enamel coated except for the tip, as a ground electrode. The ground electrode was located very close to the impaling point of the microelectrode.

Stimulus

The muscle fiber was stimulated by a short (0.05-ms), transversely applied current pulse through the two platinum plates flanking the muscle fiber. The current intensity used was, unless otherwise noted, twice the threshold value. The current was supplied through a power operational amplifier (model 440A, Opamp Labs Inc., Los Angeles, Calif.).

Characteristics of the Systems

The incident intensity of the illumination at the fiber level depends on the wavelength (λ) and the half-height width (HW) of the interference filter: it ranged from 6 to 50 mW/cm^2, and was 25 mW/cm^2 with the interference filter $\lambda = 702$ (HW 12) nm and a band pass filter KG3 (measured with a calibrated photodiode, model PIN-5DP, United Detector Technology, Santa Monica Calif.).

The frequency response of the optical recording system was measured by a light emitting diode (Hewlett-Packard Co., Palo Alto, Calif.), which emits light with a rise time of 50 ns. The overall time constant of the optical recording system was 25 μs. The response time constant of the electrical recording system for the intracellular electrode, limited by the low-pass filter, was about 30 μs.

Unless otherwise noted, the illuminating light was unpolarized: the polarization factor, P, was 0.09. ($P = (I_1 - I_2)/(I_1 + I_2)$, in which I_1 and I_2 are the maximum and minimum light intensity obtained by turning an analyzer.) In experiments using polarized light (Fig. 8), the polarization was nearly perfect ($P = 0.98$).

Merocyanine 540 Experiments

The methods so far described apply only to merocyanine rhodanine (WW375) experiments or merocyanine oxazolone (NK2367) experiments, which were conducted intermittently from February 1977 to May 1978. However, in the experiments with merocyanine 540, which had been performed earlier (from April 1975 to September 1975), the setup was not as satisfactorily arranged as that described above. For example, the shutter was not used, the adjustable X-Y-diaphragm was not available, and we used a homemade slit which did not perfectly fit the width of each single fiber. Koehler's illumination was not employed, and the intensity of illumination was about one-fourth that described above.

Notation

I_0 is the light intensity entering the fiber. I is the intensity emerging from the resting fiber. ΔI is change in the light intensity emerging from the fiber caused by stimulation; thus, the light emerging is $(I + \Delta I)$. T is transmission of the resting fiber and equals (I/I_0). ΔT is change in transmission caused by the stimulation, equivalent to $(\Delta I/I_0)$. ΔA is absorbance change.

We shall express our results in terms of the relative changes in transmission, i.e.,

$$\frac{\Delta T}{T} = \frac{\Delta I}{I} \tag{1}$$

When $(\Delta I/I)$ is very small and when transmission changes are caused by changes in absorption (rather than changes of scattering), $\Delta I/I \doteqdot -2.3\ \Delta A$ (Waggoner, 1976).

RESULTS

Light Transmission at Rest

Values of light transmission of resting single fibers were obtained by two methods: the narrow-slit method and the wide-slit method. In the narrow-slit method the width of the slit (*XY-diaph*, Fig. 1) was 7–11 μm (in this paper the slit size is expressed in reference to the actual fiber size), and the numerical aperture of the condenser was set to a small value (0.1). The slit was placed at the central part of the fiber (see the scheme in Fig. 9). The absorption coefficient of the fiber (α) can be obtained by (Jenkins and White, 1976)

$$\frac{I_{\text{narrow}}}{I_{0,\text{ narrow}}} = \exp(-\alpha D), \tag{2}$$

in which I_{narrow} is the light intensity emerging from the fiber, $I_{0,\text{ narrow}}$ is the incident light intensity, and D is the diameter.

From the values of the absorption coefficient, transmission of a whole fiber, T_f, can be calculated, assuming the fiber to be a cylinder:

$$T_f = \frac{1}{a}\int_0^a \exp(-2\alpha\sqrt{a^2 - r^2})\, dr, \tag{3}$$

in which a is fiber radius and r is the distance from the center of the fiber. The integration of Eq. 3 was kindly given by Prof. Sergio Rodriguez, Department of Physics, Purdue University:

$$T_f = \mathbf{I}_0(A) - \frac{\pi}{2}\mathbf{I}_1(A) - 2\sum_{k=1}^{\infty}(-1)^k \frac{\mathbf{I}_{2k}(A)}{4k^2 - 1}, \tag{4}$$

in which $A = 2\alpha a$, and $\mathbf{I}_0$, $\mathbf{I}_1$, etc., are the modified Bessel functions. Since Eq. 4 converges quickly, the initial three terms were enough for our purposes.

The average values of α, T_f (after stain) and α', T_f' (before stain) thus obtained are listed in Table I.

The other method is the wide-slit method, in which the resting transmission, T_f was directly measured (the condenser's numerical aperture, 0.35) by using a slit that just fit the total width of the fiber. The T_f values obtained by the wide-slit method were consistantly ~20% smaller than those obtained by the narrow-slit method. This could be due to effects such as light scattering, refraction, and the difference in the numerical apertures employed.

Transmission Changes upon Stimulation

Fig. 2 shows an example of dye absorption changes that occur upon stimulation of a single fiber. When the fiber was massively stimulated by a stimulus twice the threshold intensity, we recorded transmission changes even without staining the fiber, as shown in records *A1* and *A2*. We can distinguish two different waves, which we call wave *b* and wave *c*. In records *A1* and *A2*, wave *b* is an increase in transmission on the order of 1×10^{-3} ($\Delta I/I$), reaching a

peak about 3 ms after the start of massive stimulation (the arrows indicate the start of the stimulus). Wave *c* is a large change in transmission. The essential features of waves *b* and *c* were not altered by a color change of the incident light from 537 (*A1*) to 702 nm (*A2*). It was not possible to determine the precise wavelength dependency of waves *b* and *c*, because of their capricious nature (see below).

After records *A1* and *A2* had been taken, the fiber was stained with WW375 (100 μg/ml) for about 15 min, and transmission changes upon stimulation were again recorded. As shown in records *B1*, *B2*, and *B3*, a new optical signal (wave *a*), which started almost immediately after the stimulus, occurred. At the wavelength 702 nm, this wave is a rapid decrease in transmission (*B2* and *B3*), reaching a peak (or the lowest point) at 0.8 ms (702 nm is the wavelength

TABLE I

ABSORPTION COEFFICIENT (α) AND TRANSMITTANCE (T_f) OF RESTING FIBER STAINED WITH WW375 (NARROW-SLIT METHOD)

	Wavelength			
	840 nm	702 nm	650 nm	537 nm
α' (*before stain*, cm^{-1})	26±7	20±6	21±7	32±6
α (*after stain*, cm^{-1})	27±6	26±5	28±7	34±6
T_f' (*before stain*)	0.83±0.04	0.87±0.04	0.86±0.04	0.79±0.03
T_f (*after stain*)	0.82±0.04	0.82±0.03	0.81±0.04	0.78±0.04

Values are mean ± SEM of five fibers with an average diameter of 96 μm. Staining was carried out at 100 μg/ml for ~15 min. Sarcomere lengths were 2.6–2.7 μm. Room temperature was 24–24.5°C.

at which the maximum amplitude of wave *a* is obtained, as will be described later). Unlike waves *b* and *c*, the direction of wave *a* is remarkably dependent on the wavelength of the light. Thus, at 702 nm wave *a* is a transmission decrease (*B2*), whereas at 537 nm wave *a* becomes an increase in transmission (*B1*). Results almost the same as those shown in Fig. 2 were obtained with the fiber stained with NK2367, except for a small difference in the wavelength dependency of the signals (see below).

Because wave *a* is the only signal that appeared after the staining, and because it is the only signal that is markedly dependent on the wavelength, it seems that only wave *a* represents the absorption change of the dye. In the squid axon stained with WW375, Ross et al. (1977) have shown that the absorption changes faithfully reflect the membrane potential changes. Thus, wave *a* probably represents a membrane potential change. Since the muscle fiber was stained externally by a nonpermeant dye, the potential change upon stimulation would be the muscle action potential. Hence, we shall sometimes call wave *a* the optical action potential.

Waves *b* and *c* probably are changes in light scattering, reflecting fiber

movements. They exist before the fiber is stained, and do not show a conspicuous dependency on the wavelength. Wave *b* starts early and reaches the peak on the average at 2.3 ms. In most cases wave *b* is an increase in $\Delta I/I$ on the order of 10^{-4}–10^{-3}. On rare occasions wave *b* was absent or showed reversed polarity; the latter might have been caused by a slight injury in some part of the fiber. Even with the same fiber, the magnitude of wave *b* changed

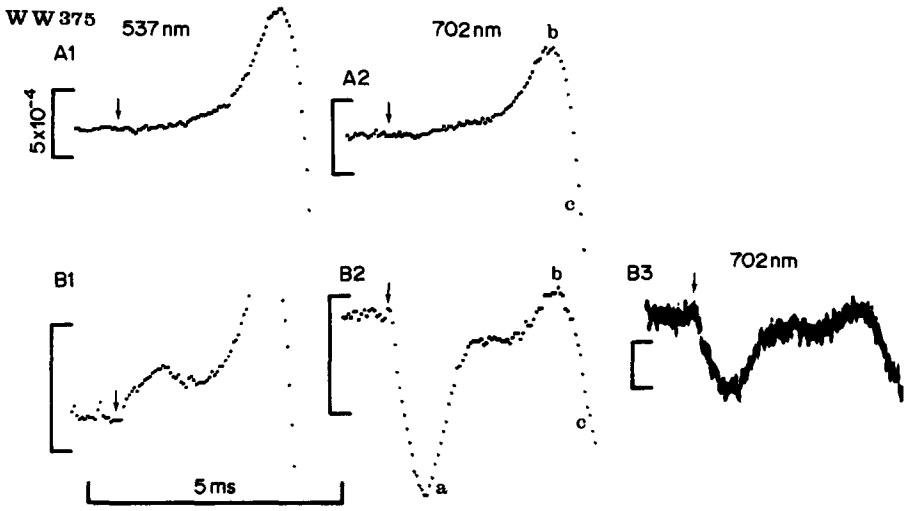

FIGURE 2. Transmission changes of an isolated single muscle fiber produced by massive stimulation. Upward direction corresponds to transmission increase. The calibration bars (5×10^{-4}) refer to $\Delta I/I$. *A1* and *A2*: before staining. *B1–B3*: after staining with WW375 (100 μg/ml) for about 15 min. Wavelength of the light was 537 nm in *A1* and *B1*, and 702 nm in *A2*, *B2*, and *B3*. Signals were averaged nine times in *A1*, *A2*, *B1*, and *B2*. A single-sweep record is shown in *B3*. Slit size = (fiber width) × 500 μm, referring to the actual fiber size. Arrows indicate the start of massive stimulation. Fiber diameter was 111 μm. Sarcomere length was 2.7 μm. Room temperature was 24.5°C. In all the optical records of this paper, the overall response time constant was ~25 μs. Unless otherwise noted, the records are photographs of an oscilloscope connected to the output of an averager (Fabri-Tek Instruments Inc., Madison, Wis.).

substantially during the course of the experiment. We think that wave *b* is a reflection of the latency relaxation, although it would at present be impossible to eliminate other causes altogether. The latency relaxation is not an infinitesimally small event (~0.3–0.5% of the twitch force; Matsumura [1969]; Mulieri [1972]; Gilai and Kirsch [1978]), and it would be surprising if we could not detect any latency relaxation by the extremely sensitive optical method. Wave *c* is a huge change in transmission following wave *b*, and is, without a doubt, caused by twitch movement of the muscle fiber.

When the fiber was stained with merocyanine 540, we obtained optical

signals similar to the ones recorded with WW375, having waves *a*, *b*, and *c* (Nakajima et al., 1976). Although we did not investigate it systematically, the wavelength dependency of wave *a* in merocyanine 540–stained fibers was completely different from that of WW375- or NK2367-stained fibers. The fiber tended to deteriorate quickly, possibly by photodynamic action.

When the fiber was treated with tetrodotoxin (TTX), all the transmission changes upon stimulation disappeared altogether, indicating that all the transmission changes observed in normal fibers were initiated by the action potential.

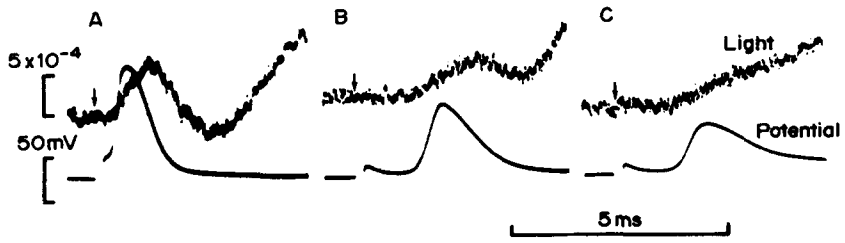

FIGURE 3. Simultaneous recordings of optical signals (upper beam) and intracellularly recorded action potentials (lower beam). The fiber was stimulated once every 2 s with the electrode kept inside the fiber, and the fiber was gradually damaged. *A* is at the fresh stage. In *B* and *C*, the fiber was damaged. Note the disappearance of distinct wave *a* when deteriorated. The fiber was stained with WW375 (100 μg/ml) for 15 min. The optical calibration refers to the value of $\Delta I/I$. In this figure, the upward direction of optical signals corresponds to transmission decrease (which is the opposite of other figures in this paper). The wavelength was 702 nm. Single-sweep records on an oscilloscope were photographed. Slit size = (fiber width) × 500 μm. Arrows indicate the beginning of massive stimulation. Fiber diameter, 114 μm. Sarcomere length, 2.7 μm. Room temperature, 24°C. The response time constant of the optical system was ~25 μs, and that of the electrical system was ~30 μs.

Fig. 3 shows records of the optical changes (wave *a*) at 702 nm (upper beams) taken simultaneously with the electrical action potential (lower beams) in an isolated single fiber. The optical signals were, as was routinely done, recorded from an area comprising a 500-μm length and the whole width of the fiber. The electrical signal was obtained through a microelectrode inserted inside this area. At 702 nm wave *a* shows a decrease in transmission. The optical signals shown in Fig. 3 were recorded in the opposite polarity from the other figures in this paper to facilitate the comparison of action potential and wave *a*.

When the fiber was fresh (Fig. 3 *A*), the microelectrode registered a large action potential (120 mV amplitude), and the optical signal revealed distinct waves *a*, *b*, and *c*. The fiber was then stimulated once every 2 s and gradually deteriorated (because the electrode remained inside while the fiber was

twitching), resulting in a loss of action potential height (Fig. 3 *B* and *C*). It can be seen in record *C* that a small and slow action potential is accompanied by a slow transmission change, in which no distinct wave *a* can be defined.

Many isolated single fibers of *Xenopus*, even if they were fresh and showed brisk twitches, did not reveal a distinct wave *a*. These fibers, whenever electrical recording was conducted, revealed small and slow action potentials. Conversely, we never failed to record a distinct wave *a* in the optical record whenever a large electrical action potential (more than 113 mV) was obtained. Therefore, we regard the presence of a distinct wave *a* as a reliable sign of a very healthy fiber. We subjected a total of 67 isolated fibers, which were seemingly healthy, to experiments with WW375 and NK2367. Of these fibers,

TABLE II

CHARACTERISTICS OF WAVE *a*

Dye	Number of fibers	Diameter	Sarcomere length	$\Delta I/I$	Time to peak	Filter wavelength
		μm	*μm*	10^{-4}	*ms*	*nm*
Merocyanine 540	9	136±20	2.5±0.2	5.7±1.6	1.51±0.61	519
WW375	18	114±16	2.7±0.1	5.7±1.7	0.93±0.16	702
NK2367	5	98±23	2.7±0.2	5.9±1.1	0.81±0.03	680

Values are mean ± SD. Time to peak was measured from the start of the massive stimulation. In merocyanine-540 experiments the fibers were stained for 8–15 min at 5 μg/ml, and the width of the slit usually did not coincide perfectly with the fiber width. A correction was made for this error. The length of the slit was either ~500 μm or 1 mm. Room temperature was 22–25°C.

In WW375 and NK2367 experiments, the fibers were stained for ~15 min at 100 μg/ml. Slit size (referred to the actual fiber) = 500 μm × (fiber width). Usually, the first measurement after the staining was made with the wavelength at the maximal signal size (702 nm with WW375 and 680 nm with NK2367). A few, however, of the measurements at these wavelengths (702 and 680 nm) were not made immediately after staining. In this case, a correction was made for the fading effect. Average room temperature was 24.7°C.

24 were eliminated from analysis because the optical record showed either no distinct wave *a* or showed a wave *a* which started after a long delay (>0.36 ms).

Table II compares the characteristics of wave *a* in fibers stained with the three dyes. In the WW375 and NK2367 experiments, only the fibers stained at 100 μg/ml for about 15 min were listed. The wave lengths were the ones for which the maximum size of wave *a* could be obtained for each dye; namely, 702 nm for WW375 and 680 nm for NK2367. It can be seen that the characteristics of wave *a* (the size as well as time to peak) in WW375 and in NK2367 experiments were very similar. Ross et al. (1977) expressed their results in terms of $(\Delta A'/A'_r)$, which is, according to them, equivalent to "the change in transmitted intensity divided by the reduction in resting transmission due to staining by the dye," i.e., $(\Delta A'/A'_r) = -\Delta T/(T_{r,\text{before}} - T_{r,\text{after staining}})$ (page 151 of Ross et al., 1977). Our data (Table II) indicate that the value of $\Delta I/I$ in WW375 experiments is 5.7×10^{-4}, which would be equivalent

to 11.4×10^{-3} in the unit of $\Delta A'/A'_r$ (calculated from the values of α and α' in Table I and the average diameter (114 μm) in Table II).

Since the action potential height in these muscle fibers was probably ~130 mV (see Table I of the following paper), $\Delta A'/A'_r$ for 50 mV depolarization becomes 4.4×10^{-3}. In the squid giant axon, stained with WW375, the value of $\Delta A'/A'_r$ for 50 mV depolarization is about -5×10^{-4} (Ross et al., 1977). Thus, the magnitude of the absorption signal in muscle is nine times as large as that in the squid axon. Similarly, in cardiac muscle, Morad and Salama (1979) obtained a large absorption value in terms of the unit ($\Delta A'/A'_r$). One of the reasons for this large value in muscle would be that in muscle fibers almost all the membranes that are stained by the externally applied dyes are excitable; whereas in the squid axon the Schwann cell membranes are also stained, which would artifically increase the denominator of ($\Delta A'/A'_r$).

Table II also shows data on merocyanine 540. The wavelength listed (519 nm), which was routinely used, is not the wavelength for the maximum absorption change. In experiments on four fibers, the magnitude of $\Delta I/I$ at 575 nm was 25% larger than that at 519 nm. Nevertheless, the data in Table II show that merocyanine 540 gives a wave *a* of roughly the same size as WW375 or NK2367.

Dose-Response Relation

Fig. 4 shows the effect of concentration of WW375 on the magnitude of wave *a*. We started with staining at a low concentration (5 or 10 μg/ml), and then the optical record was taken at 702 nm (the wavelength that gives the maximum wave *a*). This was followed by staining with higher dye concentrations. Because the dye bleaches fairly quickly (more about this in the next section), each optical measurement was performed within a few minutes after the staining. Fresh solutions of different concentrations were made from undissolved dye just before the staining. Fig. 4 *B–D* shows that the rising phases of wave *a* at different dye concentrations are almost the same, reaching the peak at 0.75–0.85 ms after the stimulus. The falling phases of wave *a* are considerably different from each other, but this would be caused by the fact that a small wave *a* obtained at a low dye concentration is more affected by the beginning of wave *b*. Fig. 4 *A* indicates that the magnitude of wave *a* probably reaches the maximum level at 100 μg/ml, and the half-effective concentration is about 10 μg/ml.

Fading of Optical Signal

The dye solutions (both WW375 and NK2367) left inside a beaker gradually lose their color. Also, after the fiber is stained, the size of wave *a* diminishes as time passes. This dwindling of wave *a* might, as Ross et al. (1977) postulated, mainly be due to dye bleaching; but dye detachment from the membrane and a diminution of action potential height resulting from fiber deterioration could also be contributing factors. The speed of the dwindling of wave *a* would depend on the light intensity, wavelength, and perhaps the stimulus frequency. We did not perform a systematic survey under controlled condi-

tions; however, a rough estimate of the time-course of the decline of wave *a* under our routine experimental conditions can be derived from the experiments in which the main purpose was the determination of the wavelength dependency of the optical signals (see below and Figs. 5–7). The data reveal that the amplitude of wave *a* declined during a period of 1,000 s to a level of 83% in WW375 experiments (five fibers) and to a level of 69% in NK2367

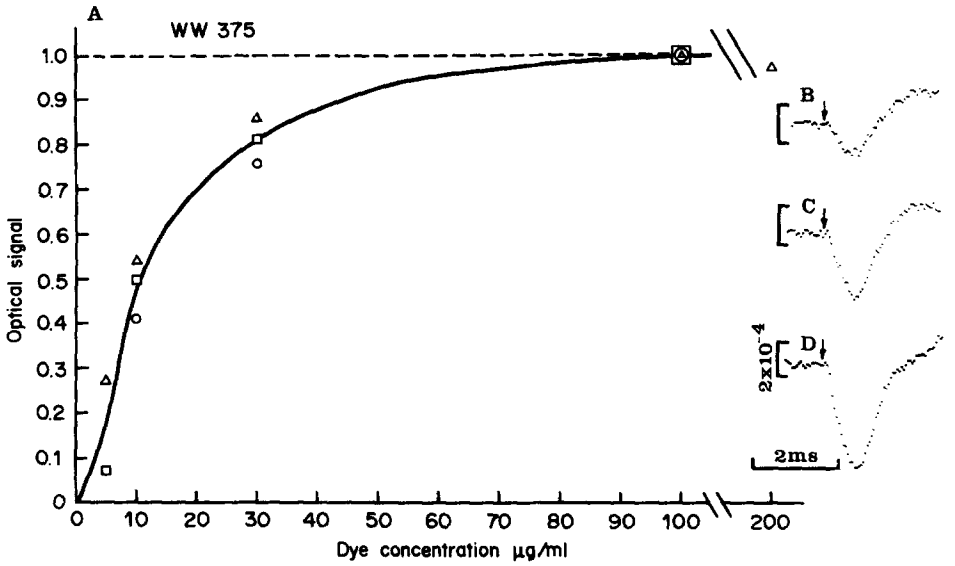

FIGURE 4. Concentration dependency of the optical signal. *A*, the height of wave *a* vs. dye concentration (WW375); the height was normalized to the value at 100 µg/ml concentration. Three fibers, corresponding to the three different symbols, were used. The fiber was first stained at a low concentration, the optical signal was recorded; then the fiber was stained at a higher dye concentration, and the procedure was repeated. For each staining, the dye was dissolved afresh, and the staining period was ~15 min. The wavelength was 702 nm. The slit size = (fiber width) × 500 µm. The diameter of the fibers was 95–126 µm. Sarcomere length was 2.6–2.7 µm. Room temperature, 25–26°C. *B–D*, are examples of wave *a* in one of the fibers at three dye concentrations: *B*, 5 µg/ml, *C*, 10 µg/ml; *D*, 100 µg/ml. Averaged nine times. The calibrations refer to $\Delta I/I$. Transmission increase, upward direction. Arrows indicate the beginning of massive stimulation.

experiments (four fibers). During these experiments the fibers were illuminated on and off with various wavelengths of light, and the average illumination over the 1,000-s period was ~4 mW/cm^2.

Spectral Characteristics of Wave a

Fig. 5 shows examples of wave *a* at vaious wavelengths in a fiber stained with WW375. On the basis of such experiments on five fibers, we plotted the

magnitude of wave *a* as a function of wavelength, as shown in Fig. 6. In plotting Fig. 6 we corrected for the fading (or bleaching effect) of wave *a*. Several measurements at different wavelengths were bracketed by measurements at a reference wavelength. We chose 720 nm or 702 nm as the reference wavelength in WW375 experiments (we chose 720 or 680 nm for NK2367 experiments). The magnitudes of wave *a* (in the unit of $\Delta I/I$) were normalized to those at 720 nm and are plotted in Fig. 6 (the left ordinate). The right ordinate was calculated from the average magnitude of $\Delta I/I$ at 702 nm measured at the initial phase of each experiment. The same experiments were performed with NK2367 on five fibers, and the results are illustrated in Fig. 7.

As seen in Fig. 2, wave *a* overlaps the initial part of wave *b*; this produces some error in the measurement of the height of wave *a*. We have analyzed wave *b* recorded before staining in nine fibers and found that this error would

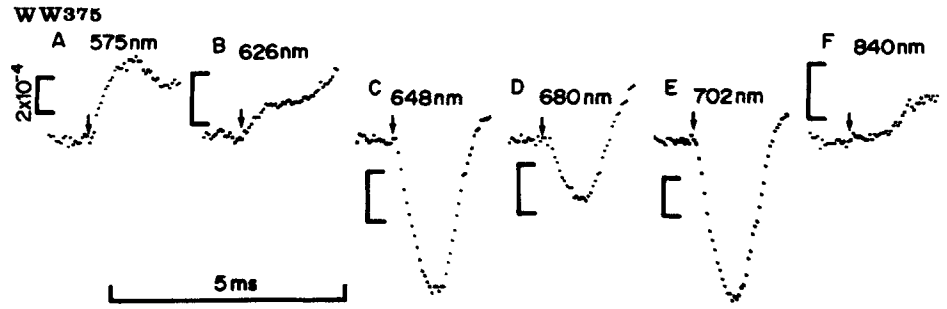

FIGURE 5. Wave *a* at various light wavelengths. Staining was with WW375 (100 μg/ml) for ~15 min. Transmission increase, upward direction. Calibrations refer to $\Delta I/I$ (2×10^{-4}), and they are not corrected for the fading effect. Averaged nine times. Slit size = (fiber width) × 500 μm. Arrows indicate the beginning of stimulus. D = 119 μm. Sarcomere length, 2.6 μm. Room temperature, 24°C.

amount to 2×10^{-5} ($\Delta I/I$). Thus, this is the magnitude of the systematic error caused by the presence of wave *b* in the spectrum curves of wave *a* shown in Figs. 6 and 7.

Figs. 6 and 7 show that the spectral characteristics of wave *a* in WW375 and in NK2367 experiments are remarkably similar, reflecting the close similarity of the chemical formulas (Waggoner, 1979). An important difference is that the spectrum with NK2367 is shifted toward the left by ~30 nm in comparison to that in WW375. In both cases, the spectrum shows a triphasic pattern, wave *a* being a decrease in transmission over the middle range of wavelengths (with WW375 over the range of 630 to 730 nm, and with NK2367 over 595 to 700 nm) and an increase in transmission outside this middle range. It can also be seen that there are two narrow peaks in the middle range, the largest peak occurring at 700 nm with WW375 (at 680 nm with NK2367) and the second peak at 650 nm with WW375 (at 625 nm with NK2367).

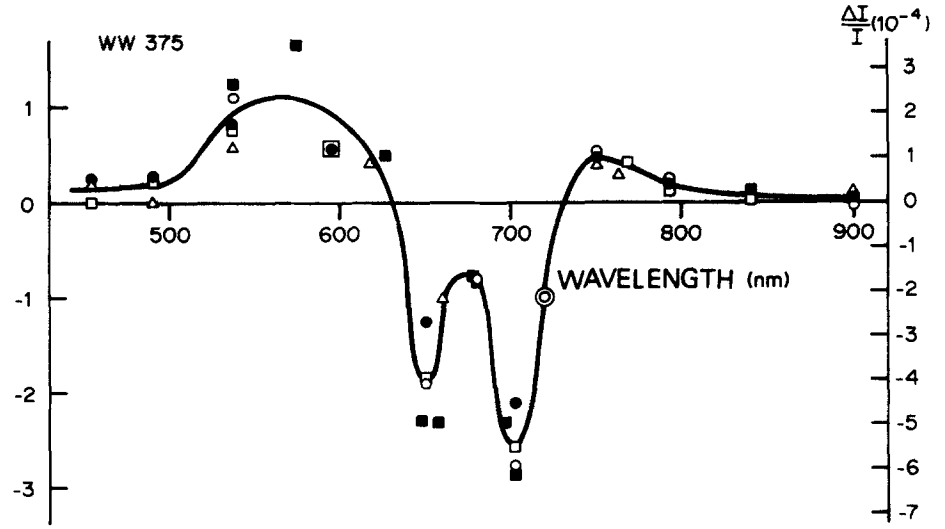

FIGURE 6. Spectral characteristic of the height of wave *a*. Staining was with WW375 (100 μg/ml) for ~15 min. Experiments on five fibers, corresponding to the five different symbols. Transmission increase corresponds to the positive direction of the ordinate. Always averaged nine times. Slit size = (fiber width) × 500 μm. Fiber diameter, 111–150 μm. Sarcomere length, 2.5–2.7 μm. Room temperature 24–25°C. The gradual fading of signal (partly due to bleaching) as well as variations of individual fibers were corrected as follows: Measurements at several different wavelengths were always bracketed by measurements at a wavelength of either 720 nm or 702 nm. Then, all the values for each fiber were normalized to the value at a standard wavelength (720 μm) of the fiber. These normalized values are indicated on the left ordinate. The right ordinate was calculated from the average of values of $\Delta I/I$ at 702 nm measured at the initial phase of each experiment (i.e., before the fading). (One fiber was excluded from this average: in this fiber the measurement at 702 nm was not made.) The continuous curve was drawn by eye.

An interesting point that emerges from Figs. 6 and 7 is that the wavelength dependency of the optical action potential is different from that of the squid axon.[1] In the axon stained with WW375, Ross et al (1977) reported that the wavelength dependency is monophasic, showing always a transmission increase over the whole range tested (450–900 nm). Thus, the results in Figs. 6 and 7 were a surprise for us, since we thought that membranous phenomena in muscle should be qualitatively the same as in the giant axon. (This triphasic

[1] We have expressed our results in terms of $\Delta I/I$. Thus, the spectrum we plotted is not equivalent to that of Ross et al. (1977) for the squid axon. They plotted the absorption change (their absorption change is different from absorbance change but is equivalent to $-\Delta I$) corrected for the wavelength-dependent efficacy of the apparatus. Their method is equivalent to plotting the results in terms of $\Delta I/I_0$ instead of $\Delta I/I$ (I_0: incident light intensity, I: emerging light intensity). As shown in Table I, I/I_0 is not very dependent on the wavelength (i.e., the resting fiber does not have a strong color). Therefore, the shape of the spectrum would be virtually the same whether we plot it in terms of $\Delta I/I$ or in terms of $\Delta I/I_0$.

pattern in muscle was reported by Baylor and Chandler (1978) and by Nakajima and Gilai (1977)).

Time-Course of Wave a at Various Wavelengths

Table II shows that wave *a* reaches its peak (peak time) at 0.95 or 0.81 ms after the stimulation in fibers stained with WW375 or with NK2367. These

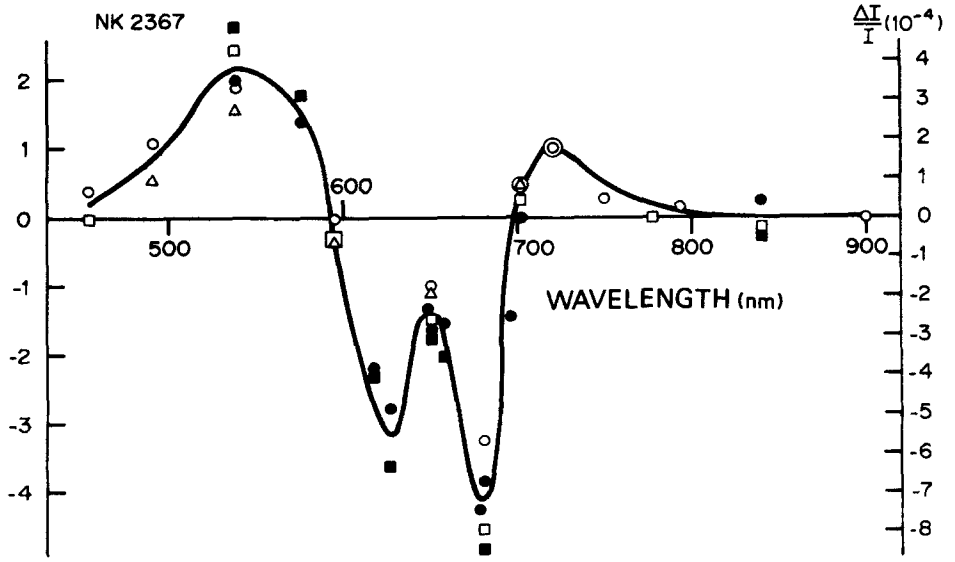

FIGURE 7. Spectral characteristics of the height of wave *a*. Staining was with NK2367 (100 μg/ml, ~15 min). Data from five fibers, represented by the five different symbols. Transmission increase, upward direction. Averaged either four or nine times. Slit size = (fiber width) × 500 μm. D = 85–116 μm. Sarcomere length, 2.5–2.9 μm. Room temperature, 24–25.5°C. The spontaneous fading of signal and variations of individual fibers were adjusted in the following way: Measurements at several different wavelengths were bracketed by measurements at the wavelengths of 720 or 680 nm. For each fiber the values were normalized to the value at 720 μm. These normalized values were plotted and are indicated on the left ordinate. The right ordinate was calculated from the average of the value of $\Delta I/I$ at 680 nm at the initial phase of each experiment. (One fiber, in which the measurement at 680 nm was not conducted, was excluded from the average.) The continuous curve was drawn by eye.

values were obtained by using the wavelengths at which the maximum response of wave *a* was elicited (702 nm with WW375 and 680 nm with NK2367). Fig. 5 shows that the peak time of wave *a* is not very dependent on the wavelength of the light. We have compared the peak times at three different wavelengths for four fibers stained with WW375 (fibers illustrated in Fig. 6). The values were 0.87 ms at 702 nm, 0.89 ms at 650 nm, and 0.96 ms at 537 nm. The small increase in peak time at 537 nm is probably caused by

the small magnitude of wave *a* at this wavelength. (Fig. 2 *B1*), and thus the wave shape is substantially influenced by the incipient wave *b*. Similar results were obtained in the NK2367 experiments. In conclusion, there is no evidence that the time-course of wave *a* depends on the wavelength of the light. Nor was the time-course of fibers stained with WW375 different from the time-course of those stained with NK2367.

Table II also shows that the time-course of wave *a* in fibers stained with merocyanine 540 was slower (peak time, 1.51 ms). This result suggests some fiber deterioration by the photodynamic action of this dye.

Dichroism

Ross et al. (1977) observed that the absorption changes in squid axons stained with WW375 are dichroic. They showed that with light polarized parallel to the long axis of the axon, the spectrum of the depolarization-induced signal was monophasic, showing a transmission increase over the whole range of wavelengths. On the other hand, when measured with light polarized perpendicular to the axis, a triphasic spectrum was obtained, showing a transmission decrease over a middle wavelength range and a transmission increase outside of this range.

The spectral pattern we obtained from muscle (Figs. 6 and 7) using unpolarized light shows some resemblance to the result on the squid axon measured with perpendicularly polarized light (although the squid axon data do not show two peaks over the middle range). Thus, it is of interest to investigate the effects of polarization on muscle fibers. In Fig. 8, we plotted the spectral pattern of wave *a* in muscle fibers illuminated by polarized light. It can be seen that the change of polarization direction has some effects on the spectral pattern of wave *a*: when illuminated by perpendicularly polarized light, there is a moderate decrease in the magnitude of $(\Delta I/I)$ over the middle range and an increase outside this range. However, this dichroism of wave *a* in muscle fibers is far less pronounced than that in the axon; in neither direction of polarization can we see the monophasic spectral pattern of the axon type. (In Fig. 8 the two sharp peaks over the middle wavelength range, which were seen in Fig. 6, are not present. This is because when the polarization experiments were performed we did not have many interference filters.) Thus, in muscle the spectrum of wave *a* shows a triphasic pattern with either unpolarized or polarized light.

Edge or Center Experiments

There is, thus, a difference in the dye-absorption properties between the muscle and the squid axonal membranes. However, since the T system comprises a large membranous area in muscle, the difference could be due to the membrane properties of the T system, and the properties of the muscle *surface* membrane might be the same as those of the axonal membrane. To answer this question we have tried to extract the optical property of the surface membrane only.

In the experiments shown in Fig. 9, the width of the slit (*XY-diaph* of Fig. 1) was decreased so that the light coming from only a narrow band of tissue

(500 μm length and 12 μm width) was recorded. Record *A* (at 702 nm) was obtained when the slit was placed at one edge of the fiber image (see the figure *inset*), and records *B1* (at 702 nm) and *B2* (at 537 nm) were obtained from the other edge of the fiber. *C1* (702 nm) and *C2* (537 nm) were obtained with the slit located at the center of the fiber image. It can be seen that wave *a* obtained from the edge (*A1* and *B1*) is fast, reaching the peak about 0.7 ms

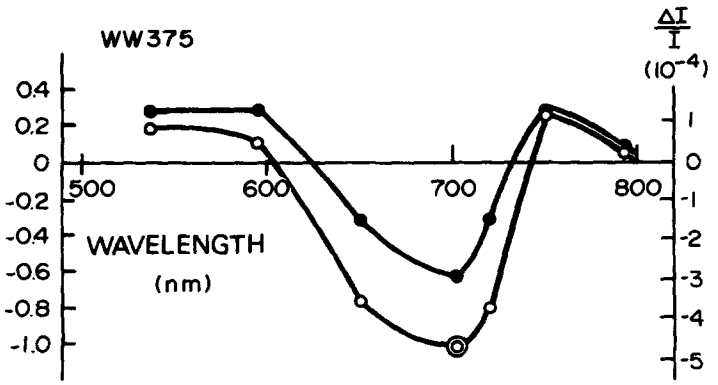

FIGURE 8. Spectral characteristics of the height of wave *a* obtained by polarized light. Staining was with WW375 (100 μg/ml, ~15 min). (○) Polarized parallel to the fiber long axis. (●) Polarized perpendicular to the fiber axis. Data represent averages obtained from three fibers. Transmission increase, upward direction. Averaged 9–36 times. Slit size = (fiber width) × 500 μm. D = 85–150 μm. Sarcomere length, 2.7–3.1 μm. Room temperature, 24°C. Measurements at several different wavelengths were bracketed by measurements with a standard light (at 702 nm with a parallel polarized light): the data were normalized to the values at the standard light. Then, the values for each wavelength were averaged. These normalized values are indicated on the left ordinate. The right ordinate was obtained through the average value of $\Delta I/I$ at 702 nm (polarized parallel) obtained at the initial phase of each experiment. (In one case the fiber was first used for another kind of experiment, and the measurement at 702 nm, polarized parallel, was made 30 min after the staining with WW375. Thus, the value was corrected for the fading effect.) The continuous curve was drawn by eye. The reason that the curve is more rounded than that in Fig. 6 is simply that the polarization experiments were carried out with a smaller number of interference filters.

after the stimulus, whereas wave *a* from the center of fiber is slower, reaching the peak 1.1 ms after the stimulus.

The muscle action potential propagates radially from the surface into the axial part of the fiber through the T system (Huxley and Taylor, 1958; Costantin, 1970; Costantin and Taylor, 1971; Bastian and Nakajima, 1974), and this is the reason why wave *a* recorded from the edge is very fast. In fact, the time-course of wave *a* from the edge is as fast as the intracellularly recorded action potential; the latter represents the potential change in the surface

membrane. On the other hand, when the slit is located at the center, the tubular membrane located at all the depths contributes to the optical signal, thus making the time-course of wave *a* slower. Detailed analysis of the time-course of wave *a* will be given in the following paper (Nakajima and Gilai, 1980).

From the inset scheme of Fig. 9, it can be seen that when the slit is placed at the edge, the contribution of the surface area to the optical signal is larger

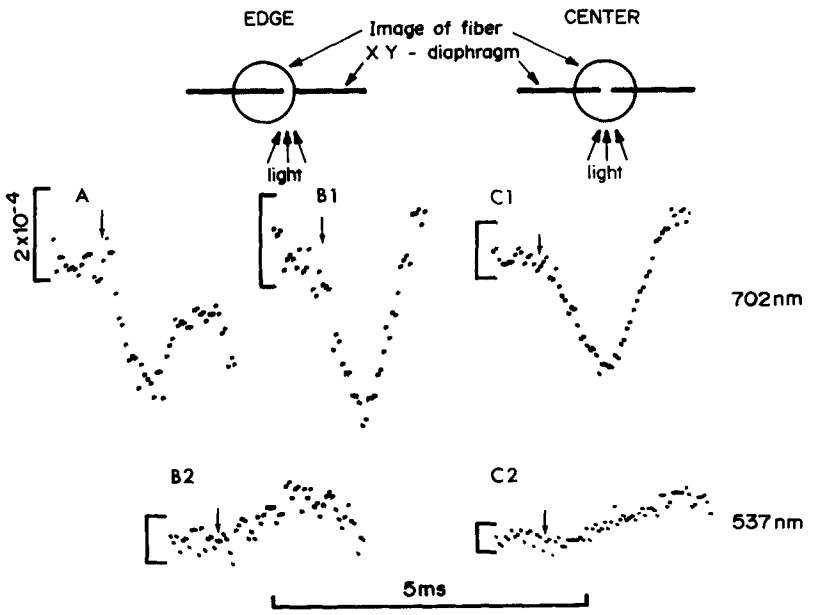

FIGURE 9. Wave *a* recorded from the edge or the center of a fiber through a narrow slit. The inset diagram explains the position of the slit in reference to the fiber image. *A* was recorded from an edge. *B1* and *B2* from the other edge. *A* and *B1* at 702 nm. *B2* at 537 nm. *C1* and *C2* recorded from the center part of the fiber. *C1* at 702 nm. *C2* at 537 nm. Staining was with WW375 (200 μg/ml, ~15 min). Transmission increase, upward direction. Calibrations refer to $\Delta I/I$. Averaged 64 times. Slit size (12 × 500 μm) referred to the actual fiber dimension. Arrows indicate the beginning of the massive stimulus. Fiber diameter, 135 μm. Sarcomere length, 2.5 μm. Room temperature, 24.5°C.

than when the slit is located at the center. From morphometric data (i.e., 0.22 μm^{-1} for the T-system area per fiber volume; Mobley and Eisenberg [1975]; cf. Peachey [1965]), we find that the surface membrane comprises 37% of the total membrane area when the slit is located at the edge, whereas the surface membrane occupies only 6% when the slit is located at the center. It can be seen from Fig. 9 that, in spite of this difference in the contribution of the surface membrane, wave *a* is always directed downward at 702 nm and always directed upward at 537 nm. We have calculated the ratio of the magnitude of

wave *a* at 702 nm to that at 537 nm. In one fiber, the ratio at the edge was 2.0 and that at the center was 2.5. In another fiber, the corresponding figures were 5.9 and 3.8. Thus, there seems to be no marked and consistent difference in this ratio between the edge and the center.

The signal-to-noise ratios are small in these experiments. Wave *a* at 537 nm is not well defined because of the overlapping of the beginning part of wave *b*. Nevertheless, the experimental results suggest, although somewhat unconvincingly, that the spectral characteristics of the surface membrane, to the extent revealed by the measurement at the two wavelengths, are not markedly different from those of the T system. If the surface membrane had a spectral characteristic of the squid axon type, wave *a* of the surface at 702 nm would have been directed upward, and thus at the edge of the fiber, where there is a substantial contribution from the surface membrane, wave *a* at 702 nm would have been directed upward or at least would have become very small.

Pulse-Staining

By staining the fiber only briefly (pulse-staining), we wished to stain predominantly the surface membrane, not the tubular membranes. The results of the pulse-staining experiments have been reported in preliminary accounts (Nakajima and Gilai, 1977 and 1978). However, wave *a* obtained by this method was small, and its time-course was not defined precisely because of an overlap with the incipient part of wave *b*. Thus, we have decided not to report the data in detail. Nevertheless, the results were not in conflict with those of the edge-center experiments.

DISCUSSION

The present paper has dealt mainly with the absorption changes accompanying action potentials of single muscle fibers stained with nonpermeant dyes, merocyanine rhodanine (WW375) and merocyanine oxazolone (NK2367), two of the best fast potential-sensitive dyes now available. The characteristics of these two dyes as potential probes are remarkably similar, and both seem to have far less toxicity than the old dye, merocyanine 540.

One interesting result of the present study is that the spectral characteristic of the optical action potential in muscle stained with WW375 or NK2367 is different from that reported in the squid giant axon (Ross et al., 1977). Using unpolarized light we observed a triphasic spectrum in muscle. By contrast, using unpolarized light, Ross et al. (1977) observed in the squid axon a monophasic spectrum. Since the T-system membrane area is much larger than the surface membrane area, we suspected that this difference in the spectral pattern is due to the presence of the tubular membrane in muscle, and that the spectrum of the muscle surface membrane might not be different from that of the axonal membrane. But this idea does not agree well with the results using a narrow slit located at the edge of the fiber image. We planned these experiments to preferentially show the properties of surface membrane. The results, although leaving some ambiguity, suggest that the surface membrane has the same kind of spectrum as the T-system membrane. Thus, both

the T system and the surface membrane seem to differ from the squid axonal membrane in their spectral pattern of the dye-absorption signals.

Recently, Ross and Reichart (1977 and 1979) studied the spectral pattern of the dye-absorption signals (WW375 and NK2367) in various neuronal materials. According to them, materials derived from invertebrate animals showed the monophasic pattern of the squid axon type, whereas neurons obtained from vertebrates showed the triphasic pattern. But the generalization may not be valid, because in cardiac muscle of vertebrates Morad and Salama (1979) found a triphasic pattern with WW375 but not with NK2367. Also, S. M. Baylor, W. K. Chandler, and M. W. Marshall,[2] using plane-polarized light, observed both monophasic and triphasic spectra with WW375 in the frog skeletal muscle under conditions different from ours.

The precise mechanisms of the origin of the dye-absorption changes induced by membrane polarization are not known. One theory proposes that there is a shift of dye monomer-dimer equilibrium inside the membrane (Tasaki et al., 1974; Ross et al., 1974 and 1976; Tasaki and Warashina, 1976; Waggoner and Grinvald, 1977; Waggoner, 1979). Tasaki and Warashina (1976) and Waggoner and Grinvald (1977) measured the absorption spectra of monomers and dimers of merocyanine 540. On the basis of these spectral patterns, they were able to reconstruct a spectrum of absorption changes by assuming monomer-dimer equilibrium and by assuming that the monomer absorption moments are more perpendicular to membrane surface.

The triphasic spectral pattern of dye-absorption changes in muscle stained with WW375 or NK2367 (Figs. 6 and 7), as well as the dye-absorption characteristics produced by the changes in polarization direction, resembles the results obtained in the merocyanine 540–stained squid axon (Ross et al., 1977). This suggests that a monomer-dimer equilibrium shift similar to that proposed for the axon stained with merocyanine 540 can explain all the results reported in the present paper. But obviously this mechanism cannot explain the monophasic spectrum obtained in the squid axon stained with WW375 or NK2367. One explanation, which was proposed by Ross and Reichart (1977), is that more than one reaction, involving different states of the dyes, occurs in both the squid axon and vertebrate muscles, one reaction overshadowing others under different conditions in different materials. This hypothesis appeals to us since it does not postulate a qualitative difference among various kinds of tissues.

We thank Dr. L. B. Cohen for his unfailing advice. Thanks are also due to Dr. R. Miledi for his hospitality extended to S. Nakajma at University College London, where the manuscript was written. We are indebted to: Drs. L. H. Pinto and W. A. Cramer for their many suggestions concerning optical measurement, Dr. A. S. Waggoner for supplying the dye WW375, Dr. S. Rodriguez, Department of Physics, Purdue University, for solving Eq. 4, and Dr. F. E. Lytle, Department of Chemistry, Purdue University, for measuring the frequency response of our optical system. Many thanks to Ms. J. H. Blanchard for editing the manuscript and to Mrs. R. M. Killian for clerical help.

[2] *In* The Regulation of Muscle Contraction, Excitation-Contraction Coupling. A. D. Grinnell and M. A. B. Brazier, editors. Academic Press, Inc., New York. In press.

Supported by National Institutes of Health grant NS-08601 and a fellowship from the Muscular Dystrophy Association.

Received for publication 31 March 1980.

REFERENCES

BASTIAN, J., and S. NAKAJIMA. 1974. Action potential in the transverse tubules and its role in the activation of skeletal muscle. *J. Gen. Physiol.* **63**:257–278.

BAYLOR, S. M., and W. K. CHANDLER. 1978. Optical indications of excitation-contraction coupling in striated muscle. *In* Biophysical Aspects of Cardiac Muscle. M. Morad, editor. Academic Press, Inc., New York. 207–228.

BAYLOR, S. M., W. K. CHANDLER, and M. W. MARSHALL. 1979. Temporal comparison of different optical signals associated with E-C coupling in frog muscle. *Biophys. J.* **25**(2, Pt. 2): 119 *a*. (Abstr.).

BEZANILLA, F., and P. HOROWICZ. 1975. Fluorescence intensity changes associated with contractile activation in frog muscle stained with Nile blue A. *J. Physiol. (Lond.)*. **246**:709–735.

COHEN, L. B., D. LANDOWNE, B. B. SHRIVASTAV, and J. M. RITCHIE. 1970. Changes in fluorescence of squid axons during activity. *Biol. Bull. (Woods Hole)*. **139**:418–419.

COHEN, L. B., and B. M. SALZBERG. 1978. Optical measurement of membrane potential. *Rev. Physiol. Biochem. Pharmacol.* **83**:35–88.

COHEN, L. B., B. M. SALZBERG, H. V. DAVILA, W. N. ROSS, D. LANDOWNE, A. S. WAGGONER, and C. H. WANG. 1974. Changes in axon fluorescence during activity: molecular probes of membrane potential. *J. Membr. Biol.* **19**:1–36.

COSTANTIN, L. L. 1970. The role of sodium current in the radial spread of contraction in frog muscle fibers. *J. Gen. Physiol.* **55**:703–715.

COSTANTIN, L. L., and S. R. TAYLOR. 1971. Active and passive shortening in voltage-clamped frog muscle fibers. *J. Physiol. (Lond.)*. **218**:13P.

ECKER, A. 1971. The Anatomy of the Frog. Clarendon Press, Oxford.

GILAI, A., and G. E. KIRSCH. 1978. Latency-relaxation in single muscle fibers. *J. Physiol. (Lond.)*. **282**:197–205.

GILAI, A., and S. NAKAJIMA. 1976. Dye absorption changes during excitation of single amphibian muscle fibers. *Biophys. J.* **16**(2, Pt. 2):153 *a*.

GRINVALD, A., B. M. SALZBERG, L. B. COHEN, K. KAMINO, A. S. WAGGONER, C. H. WANG, and D. TI. 1976. Simultaneous recording from twelve neurons in the supraesophageal ganglion of *Balanus nubilus* using a new potential sensitive dye. *Biol. Bull. (Woods Hole)*. **151**:411.

HODGKIN, A. L., and P. HOROWICZ. 1959. The influence of potassium and chloride ions on the membrane potential of single muscle fibers. *J. Physiol. (Lond.)*. **148**:127–160.

HUXLEY, A. F., and R. E. TAYLOR. 1958. Local activation of striated muscle fibers. *J. Physiol. (Lond.)*. **144**:426–441.

JENKINS, F. A., and H. E. WHITE. 1976. Fundamentals of Optics. McGraw-Hill, Inc., New York.

LANDOWNE, D. 1974. Changes in fluorescence of skeletal muscle stained with merocyanine associated with excitation-contraction coupling. *J. Gen. Physiol.* **64**:5 *a*. (Abstr.).

MATSUMURA, M. 1969. On the nature of the latency relaxation of frog skeletal muscle. *Jpn. J. Physiol.* **19**:701–711.

MOBLEY, B. A., and B. R. EISENBERG. 1975. Sizes of components in frog skeletal muscle measured by methods of stereology. *J. Gen. Physiol.* **66**:31–45.

MORAD, M., and G. SALAMA. 1979. Optical probes of membrane potential in heart muscle. *J. Physiol. (Lond.)*. **292**:267–295.

MULIERI, L. A. 1972. The dependence of the latency relaxation on sarcomere length and other characteristics of isolated muscle fibers. *J. Physiol. (Lond.)*. **223:**333–354.

NAKAJIMA, S., and A. GILAI. 1977. Recording of action potential from single muscle fibers by use of potential sensitive dyes. *J. Gen. Physiol.* **70:**13 *a*. (Abstr.).

NAKAJIMA, S., and A. GILAI. 1978. Dye absorption changes in single muscle fibers. *Biophys. J.* **21**(2, Pt. 2)**:**63 *a*.

NAKAJIMA, S., and A. GILAI. 1980. Radial propagation of muscle action potential along the tubular system examined by potential-sensitive dyes. *J. Gen. Physiol.* **76**:751–762.

NAKAJIMA, S., A. GILAI, and D. DINGEMAN. 1976. Dye absorption changes in single muscle fibers: an application of an automatic balancing circuit. *Pfluegers Arch. Eur. J. Physiol.* **362:** 285–287.

OETLIKER, H., S. M. BAYLOR, and W. K. CHANDLER. 1975. Simultaneous changes in fluorescence and optical retardation in single muscle fibers during activity. *Nature (Lond.)*. **257:**693–696.

PEACHEY, L. D. 1965. The sarcoplasmic reticulum and transverse tubules of the frog's sartorius. *J. Cell Biol.* **25:**209–231.

ROSS, W. N., and L. F. REICHARDT. 1977. Species-specific effects on the optical signals of voltage-sensitive dyes. *J. Gen. Physiol.* **70:**15 *a*–16 *a*. (Abstr.).

ROSS, W. N., and L. F. REICHARDT. 1979. Species-specific effects on the optical signals of voltage-sensitive dyes. *J. Membr. Biol.* **48:**343–356.

ROSS, W. N., B. M. SALZBERG, L. B. COHEN, and H. V. DAVILA. 1974. A large change in dye absorption during the action potential. *Biophys. J.* **14:**983–986.

ROSS, W. N., B. M. SALZBERG, L. B. COHEN, A. GRINVALD, H. V. DAVILA, A. S. WAGGONER, and C. H. WANG. 1977. Changes in absorption, fluorescence, dichroism, and birefringence in stained giant axons: optical measurement of membrane potential. *J. Membr. Biol.* **33:**141–183.

TASAKI, I., and A. WARASHINA. 1976. Dye-membrane interaction and its changes during nerve excitation. *Photochem. Photobiol.* **24:**191–207.

TASAKI, I., A. WARASHINA, and H. PANT. 1974. Energy transfer between fluorescent probe molecules in and across nerve membrane. *Biol. Bull. (Woods Hole)*. **147:**501.

TASAKI, I., A. WATANABE, R. SANDLIN, and L. CARNAY. 1968. Changes in fluorescence, turbidity, and birefringence associated with nerve excitation. *Proc. Natl. Acad. Sci. U. S. A.* **61:**883–888.

VERGARA, J., and F. BEZANILLA. 1976. Fluorescence changes during electrical activity in frog muscle stained with merocyanine. *Nature (Lond.)*. **259:**684–686.

VERGARA, J., F. BEZANILLA, and B. M. SALZBERG. 1978. Nile blue fluorescence signals from cut single muscle fibers under voltage or current clamp conditions. *J. Gen. Physiol.* **72:**775–800.

WAGGONER, A. S. 1976. Optical probes of membrane potential. *J. Membr. Biol.* **27:**317–334.

WAGGONER, A. S. 1979. Dye indicators of membrane potential. *Annu. Rev. Biophys. Bioeng.* **8:**47–68.

WAGGONER, A., and A. GRINVALD. 1977. Mechanisms of rapid optical changes of potential sensitive dyes. *Ann. N. Y. Acad. Sci.* **303:**217–241.